

A preconditioning strategy for microwave susceptibility in ferromagnets

Stéphane Labbé*

November 16, 2018

Abstract

3D numerical simulations of ferromagnetic materials can be compared with experimental results via microwave susceptibility. In this paper, an optimised computation of this microwave susceptibility for large meshes is proposed. The microwave susceptibility is obtained by linearisation of the Landau and Lifchitz equations near equilibrium states and the linear systems to be solved are very ill-conditioned. Solutions are computed using the Conjugate Gradient method for the Normal equation (CGN Method). An efficient preconditioner is developed consisting of a projection and an approximation of an “exact” preconditioner in the set of circulant matrices. Control of the condition number due to the preconditioning and evolution of the singular value decomposition are shown in the results.

1 Introduction

Ferromagnetic simulation via the micromagnetic model is a real-life computational challenge. Ferromagnetic materials are used in numerous applications such as radar protection, magnetic recording or micro electronics. In these applications, the magnetic objects studied are micro or nano-objects which are difficult and expensive to craft. Thus, one of the optimisation solutions, for the shape and composition of such particles, is numeric simulation. The first step in this type of simulation is to compute the dynamic of the magnetisation and the equilibrium states. However, a direct comparison of the results with experiments is impossible for 3D particles. The main comparison tool is microwave susceptibility as the resonance numerical curves can be compared with the physical experiments. At that point several difficulties are encountered. The main one is managing a large number of degrees of freedom. This is required to compute interesting configurations with sufficient accuracy.

In this article, we use the micromagnetism model in order to model the magnetisation behaviour in ferromagnetic materials. This model is a mesoscopic model, ie. a model valid for a scale between the one used for microscopic Maxwell equations and the scale of classic macroscopic Maxwell equations. In this model, magnetisation does

*Université Paris Sud, Laboratoire de Mathématique, Bât. 425, 91405 Orsay Cedex, 33-(0)1-69-15-60-42, 33-(0)1-69-15-67-18, stephane.labbe@math.u-psud.fr

not linearly depend on magnetic excitation but is controlled by a non-linear system: the Landau-Lifschitz equation (1). This model was introduced by Brown [1, 2].

There are two ways to obtain the equilibrium states. The first by energy minimisation ([3, 4, 5]), the second by relaxation of the dynamic system ([6, 7]). The main advantage of the dynamical approach is to compute an equilibrium state linked to given initial data by a life-like dynamic process; then, we can apply dynamical treatments, via the external field, in order to find specific equilibrium states.

Computation of the microwave susceptibility can be performed by two main methods: the Harmonic Direct Computation and the Fourier Transform Method. The first method is based upon the use of a linearised version of the evolution equation perturbed by a time harmonic external field. The second is based upon the injection of an harmonic perturbation. The Fourier method implies the resolution of a time dependant problem that is quite ill-conditionned for low frequencies (the time step ensuring that the convergence vanishes swiftly when the frequency decreases) but the linearisation methods permit the range of frequencies used in the applications to be attained.

2 The microwave susceptibility problem

2.1 The linearisation

In this problem, we are interested in computing the microwave response of a ferromagnetic system to an external harmonic excitation. We consider that the ferromagnetic material is homogeneous and contained in a C^1 -class piecewise domain of \mathbb{R}^3 denoted Ω . Then, we study the evolution of the magnetisation field in the neighbourhood of an equilibrium state of the dynamic equation. This equation, in the micromagnetism model [1], is given by the Landau-Lifschitz system: find m in $\tilde{H}^1([0, T] \times \mathbb{R}^3, \Omega; \mathbb{R}^3) = \{m \in L^2(\mathbb{R}^3; \mathbb{R}^3) | \forall t \in [0, T], m|_{\Omega} \in H^1(\Omega; \mathbb{R}^3) \text{ and } m \equiv 0 \text{ in } \mathbb{R} \setminus \Omega\}$ such that

$$\begin{cases} \frac{\partial m}{\partial t} = f(m, h_{ext}) = -m \wedge (H(m) + \ell) - \alpha m \wedge (m \wedge (H(m) + \ell)), \in (0, T] \times \Omega, \\ m(x, 0) = m_0(x), \forall t \in \Omega. \end{cases} \quad (1)$$

where H is a linear operator, from $\tilde{H}^1([0, T] \times \mathbb{R}^3, \Omega; \mathbb{R}^3)$ into $H^{-1}(\mathbb{R}^3; \mathbb{R}^3)$, ℓ the external magnetic field (independent of the magnetisation and element of $L^\infty([0, T] \times \mathbb{R}^3; \mathbb{R}^3)$, α the damping factor (a strictly positive real) and m_0 is a given element of $\tilde{S}^2(\Omega) = \{m \in \tilde{H}^1(\mathbb{R}^3, \Omega; \mathbb{R}^3) | |m|_{\Omega}| = 1, \text{ a.e. in } \Omega\}$. In this model, we can see that the local module of the magnetisation is naturally preserved. In this article, we define H as follows: $\forall m \in \tilde{H}^1([0, T] \times \mathbb{R}^3, \Omega; \mathbb{R}^3)$

$$H(m) = A\Delta m + H_d(m) + K(m - (m \cdot u)u)$$

where A and K positive real constants and u is an element of $\tilde{H}^1([0, T] \times \mathbb{R}^3, \Omega; S^2)$ (S^2 designates the unit sphere). The operator H_d is defined in the sense of distributions on \mathbb{R}^3 by

$$\begin{cases} \text{rot}(H_d(m)) = 0, \\ \text{div}(H_d(m)) = -\text{div}(m). \end{cases}$$

Now, let us define the equilibrium states of the system (1)

Definition 1 For a given ℓ in $L^\infty(\mathbb{R}^3; \mathbb{R}^3)$ (independent of time), a magnetisation state m_ℓ , in $\tilde{H}^1(\mathbb{R}^3, \Omega; \mathbb{R}^3)$ is an equilibrium state if, and only if,

$$f(m_\ell, \ell) = 0, \text{ a.e. in } \Omega.$$

Then, for a given equilibrium state m_ℓ , associated to an external state ℓ , we define the microwave susceptibility

Definition 2 For a given equilibrium state m_ℓ , associated to an external field ℓ , we denote a susceptibility tensor of the order 3 complex matrices $\chi(\ell)$ defined by

$$(\chi(\ell))_{l,k} = -\frac{1}{2T}(\lambda_k, m_l)_{0,\Omega}, \quad \forall (l, k) \in \{1, 2, 3\}^2,$$

with $\lambda_k = \zeta_k e^{i\omega t}$ and ζ_k is a constant vector of \mathbb{R}^3 . Furthermore, we suppose that $(\zeta_k)_{k \in \{1,2,3\}}$ is an orthogonal basis of \mathbb{R}^3 . Then, for all k in $\{1, 2, 3\}$, m_k is a solution of (1) for the external field $\lambda_k + \ell$ and the initial data $m_0 = m_\ell$.

Formally, if the excitation ζ_k is sufficiently small, then the magnetisation responses will be also small and we can define this response for every k in $\{1, 2, 3\}$ by

$$m_k - m_\ell = \mu_k e^{i\omega t},$$

with $\mu_k \in \tilde{H}^1(\mathbb{R}^3, \Omega; \mathbb{C}^3)$. In the following we suppose that ζ_k and μ_k are of the same order.

Then, if we re-write the system (1) verified by m_k , the linearised equation gives

$$(i\omega - D_{1,\ell} \circ h - D_{2,\ell})(\mu_k) = D_{1,\ell}(\zeta_k) \quad (2)$$

where, for all w in $L^\infty(\mathbb{R}^3; \mathbb{R}^3)$, we set

$$\begin{aligned} D_{1,\ell}(w) &= -m_\ell \wedge w - \alpha m_\ell \wedge (m_\ell \wedge w), \\ D_{2,\ell}(w) &= (H(m_\ell) + \ell) \wedge w + \alpha m_\ell \wedge (w \wedge (H(m_\ell) + \ell)) \end{aligned}$$

2.2 The discretisation of the linearised equation

In order to discretise the equation, we consider a monolith $K(\Omega)$ such that $\Omega \subset K(\Omega)$. Ideally, this monolith is the smallest containing Ω . Then, $K(\Omega)$ is discretised using a regular cubic mesh of cells $(\Omega_i)_{i \in N_h}$ where h is the length of a cell and N_h is the set of the indices. We set $\Omega_h = \bigcup_{i \in N_{int,h}} \Omega_i$ where $N_{int,h} \subset N_h$ is the set of indices such that, for every i in $N_{int,h}$, $\Omega_i \cap \Omega \neq \emptyset$.

Then, we choose as a discrete space for all euclidian space F :

$$W_h(F) = \{u \in L^2(\mathbb{R}^3; F) \mid u \equiv 0 \text{ in } \mathbb{R}^3 \setminus K(\Omega) \text{ and } \forall i \in N_h, u|_{\Omega_i} \text{ is a constant}\},$$

for each u in W_h , we set: $\forall i \in N_h, u_i = u|_{\Omega_i}$. We choose the L^2 scalar product on \mathbb{R}^3 as the scalar product on W_h , we denote it $(u, v)_{0,\Omega}$ for all u, v in $L^2(\mathbb{R}^3; F)$. Then, setting

$$\begin{aligned} L^2(\mathbb{R}^3; F) &\xrightarrow{P_h} W_h(F) \\ u &\longmapsto P_h(u) = \sum_{i \in N_h} \left(\frac{\mathbf{1}_i}{h^3} \int_{\Omega_i} u \, dx \right) \end{aligned}$$

where $\mathbf{1}_i$ is defined for x in \mathbb{R}^3 by $\mathbf{1}_i(x) = 1$ if x belongs to Ω_i , $\mathbf{1}_i(x) = 0$ otherwise. P_h^* designates the canonical injection of $W_h(F)$ onto $L^2(\mathbb{R}^3; F)$.

These definitions lead to the following formulas for the discrete magnetic contributions:

$$H_{a,h} = P_h \circ H_a \circ P_h^*,$$

and

$$H_{d,h} = P_h \circ H_d \circ P_h^*,$$

the analysis of $H_{a,h}$ is straightforward. On the other hand, the analysis of $H_{d,h}$ is not direct, in particular, it has been demonstrated that this discretisation preserves the main properties of the demagnetisation operator H_d (H_d is a projection operator), and a lower estimate of its lower eigenvalue is given. Furthermore, the computation of this operator is very expensive: the discrete matrix is a full matrix. Then, to optimise its computation, we choose to use a regular cubic mesh which ensure a specific structure for the discrete operator. This block-Toeplitz structure enables us to reduce the storage of the matrix from $\#(N_h)^2$ to $O(\#(N_h))$ and the computation cost from $\#(N_h)^2$ to $O(\#(N_h) \log(\#(N_h)))$. For complete analysis of the discretisation of H_d , see [8]. The Laplacian operator is discretised using the classical 7 point scheme, the discretised operator is designated in the following by Δ_h . The total discretised magnetic field is then defined by

$$H_h(m) = A\Delta_h m + H_{d,h}(m) + H_{a,h}(m).$$

Then, for a given external field ℓ in $W_h(\mathbb{R}^3)$, we set $m_{h,\ell}$, element of $W_h(S^2)$, the equilibrium state of the discretised version of (1). This state is obtained using an explicit time discretisation combined with an optimisation of time which ensures its stability (see [9, 10, 7]). This equilibrium state, as seen previously, is such that: $\forall i \in N_h, \exists \beta_i \leq 0$ and

$$H_h(m_{h,\ell})\mathbf{1}_i = \beta_i m_{h,\ell} \mathbf{1}_i,$$

we set $H_h(m_{h,\ell}) = B_\ell(m_{h,\ell})$ where B_ℓ is a diagonal operator. Knowing an equilibrium state for the discretised system, we can define the linearised discrete system: $\forall \omega \in \mathbb{R}_*^+$,

$$(i\omega - D_{1,h,\ell}(H_h - B_\ell))\mu_h = D_{1,h,\ell}\zeta_h \quad (3)$$

where $D_{1,h,\ell}$ is the operator $D_{1,\ell}$ built for the $m_{h,\ell}$ equilibrium state.

Then, for each element u of $W_h(\mathbb{R}^3)$, we associate a unique element U of $\mathbb{R}^{3\#(N_h)}$ defined by

$$\forall i \in N_h, U_i \in \mathbb{R}^3 \text{ and } U_i = \frac{1}{h^3} \int_{\Omega_i} u(x) dx.$$

Using this bijection between $W_h(\mathbb{R}^3)$ and $\mathbb{R}^{3\#(N_h)}$, we can write a matricial version of the linearised discrete version of (1): find U_k in $\mathbb{R}^{3\#(N_h)}$ such that, for a given Y_k built on ζ_k we have

$$M_\omega U_k = D Y_k, \quad (4)$$

where, for every U in $\mathbb{R}^{3\#(N_h)}$, for every i in N_h

$$(M_\omega U)_i = \frac{1}{h^3} \int_{\Omega_i} \left((i\omega - D_{1,h,\ell}(H_h - B_\ell)) \left(\sum_{i \in N_h} U_i \mathbf{1}_i \right) \right) dx,$$

and

$$(D Y_k)_i = \frac{1}{h^3} \int_{\Omega_i} \left(D_{1,h,\ell} \left(\sum_{i \in N_h} Y_{k,i} \mathbf{1}_i \right) \right) dx,$$

For use in the remainder of this paper for every U in $\mathbb{R}^{3\#(N_h)}$ we set:

$$DHU = -M_\omega U + i\omega U$$

then H is the matrix associated to the discrete operator $H_h - B_\ell$.

2.3 Some properties of the discrete system (4)

We set M_ℓ , the element of $\mathbb{R}^{3\#(N_h)}$ associated to $m_{h,\ell}$. Let us define $[m_{h,\ell}]^\perp$ by

$$[m_{h,\ell}]^\perp = \{W \in \mathbb{C}^{3\#(N_h)} | \forall i \in N_h, M_{\ell,i} W_i = 0\},$$

and we designate by P_ℓ^\perp the projection from $\mathbb{C}^{3\#(N_h)}$ into $[m_{h,\ell}]^\perp$. Then we can demonstrate:

Theorem 1 *For every Y in $\mathbb{R}^{3\#(N_h)}$ and for every ω strictly positive, the system (4) is regular and its solution is in an element of $[m_{h,\ell}]^\perp$.*

Proof: If U is the solution of (4), then we have

$$i\omega U = D(Y_k + HU),$$

knowing that D sends elements of $\mathbb{C}^{3\#(N_h)}$ in $[m_{h,\ell}]^\perp$, we conclude that U is also an element of $[m_{h,\ell}]^\perp$.

Then, considering V in $[m_{h,\ell}]^\perp$, due to the structure of H , we have HV as an element of $[m_{h,\ell}]^\perp$. Each diagonal block (3×3) has $0, \alpha + i$ and $\alpha - i$ as eigenvalues. Knowing that the eigenvalues of H (symetric matrix) are real, we deduce that the eigenvalues of DH are complex numbers of non vanishing real parts unless the eigenvalue is null. Then, the eigenvalues of M_ω can not vanish. □

The conditioning number of the matrix M_ω can be estimated

Theorem 2 *For every ω real strictly positive, we have*

$$\text{cond}(M_\omega) \leq \sqrt{\frac{\omega^2 + (1 + \alpha^2)(1 + \frac{1}{h^3})(\frac{A}{h^2} + 1 + K)}{\omega^2}}$$

Proof: This theorem is proved using the Courant-Fisher theorem for hermitian matrices which provides formulae for the highest and lowest eigenvalues. The proof is then classical and uses the fact that D^*D is the projection matrix on $[m_{h,\ell}]^\perp$ multiplied by $(1 + \alpha^2)$.

□

We notice that the conditioning number $\text{cond}(M_\omega)$ behaves as expected when ω tends to infinity:

$$\lim_{\omega \rightarrow \infty} \text{cond}(M_\omega) = 1.$$

Here, the fact that ω grows to infinity means that it dominates $\frac{1}{h^2}$. Now, if we consider that ω is fixed, the behaviour of $\text{cond}(M_\omega)$ shows that the system is ill-conditioned

$$\lim_{h \rightarrow 0} \text{cond}(M_\omega) = \infty.$$

Thus, the pre-conditioning of the system is essential. In fact, the most interesting part of the spectrum of susceptibility for numerous applications is the low frequency part.

3 The preconditioning strategy

3.1 Choice of the inversion method

In order to solve system (4), we chose an iterative method; this choice is conditioned by the fact that the matrices considered are non-symmetric full matrices and the order of the systems to solve is great (up to 10^6). Three main iterative methods are used commonly to solve non symmetric systems:

- the normal conjugate gradient (CNG),
- the generalised minimal residual method (GMRES),
- the conjugate gradient squared (CGS).

As shown in the article of Nachtigal, Reddy and Trefethen [11], none of this three methods could be considered as a cure-all for all non-symmetric systems. As the convergence quality of CGS and GMRES is influenced by eigenvalue clustering of the system matrix, CNG method convergence depends on singular value clustering. As the preconditioning strategy presented in this article is based upon the amelioration of the singular value clustering, we chose, of course, the CNG method. Furthermore, tests not presented in this article show that the CNG method seems to be more adapted for this type of system, even if not preconditioned.

3.2 An example of singular value repartition and of CNG convergence rate

In the remainder of this paper, we have chosen to illustrate the results presented using a plain example. This example has been chosen for the low order, 192, of its system

which facilitates the visualisation (done with Matlab). The mesh chosen is a $4 \times 4 \times 4$ regular cubic mesh of a cubic domain. We set it in the dimensionless system $A = 0,88 \cdot 10^{-10}$, $K = 0,57 \cdot 10^{-2}$, $\alpha = 0,5$ and the cube length is equal to 10^{-6} . For this bench, we would want to choose ω between $\omega_{min} = 0,452 \cdot 10^3$ Hz and $\omega_{max} = 0,452 \cdot 10^5$ Hz. In Fig. 2 the error evolution for the CNG is shown. Here we have

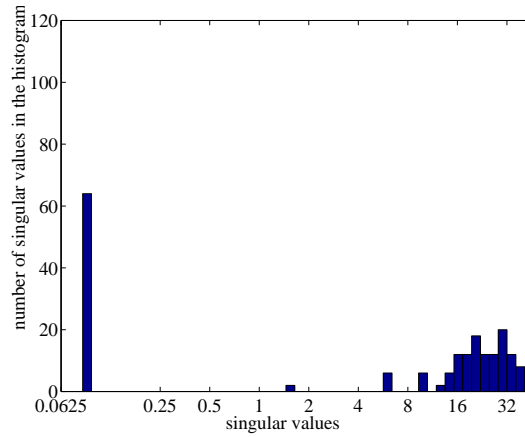


Figure 1: Singular value decomposition for the non-preconditioned system.

chosen a final error criteria of 10^{-5} . With no preconditioning, the system converges in 56 iterations for ω_{min} and 48 iterations for ω_{max} , the preconditioning number is almost equal to 7500 (slight variations between ω_{min} and ω_{max}).

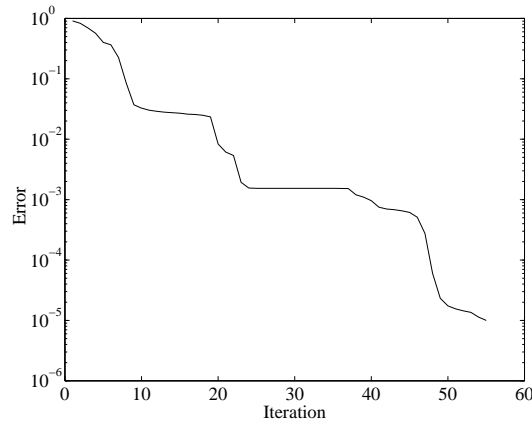


Figure 2: Residue of the CNG for ω_{min} .

3.3 The preconditioning strategy

We have three main goals to build the preconditioner:

- to use the known properties of the system,
- decrease the conditioning number sensitivity to the mesh size,
- build a cheap preconditioner (memory size and computational cost).

The first point is taken into account by using the result presented in Theorem 1: the right side of the preconditioner will be a projection on $[m_{h,\ell}]^\perp$. This first step of projection eliminates the cluster of singular values near 0 and ensures a convergence in 48 iterations for ω_{min} and of 27 iterations for ω_{max} .

3.4 The “exact” preconditioner

As a first stage, we would want to build a symmetric left preconditioner. The non symmetry of M_ω comes from the operator $D_{1,h,\ell}$. In fact, we have

$$D_{1,h,\ell} w = -m_\ell \wedge w + \alpha P_\ell^\perp w,$$

the first part of the operator is a rotation, and the second part a projection. Then, it is possible to prove that $D_{1,h,\ell}$ does not have a main influence on the singular value decomposition. This means that we may choose a left preconditioner $M_{g,\omega}$ built on the operator

$$i\omega - \alpha(H_h - B_\ell),$$

That is to say, if we set H the matrix built on the operator $H_h - B_\ell$

$$M_{g,\omega} = i\omega Id - \alpha H.$$

In the sequel, even if we do not write the projection to lighten the notations, we consider that the system is right preconditioned by P_ℓ^\perp . Then, we prove the following theorem

Theorem 3 *For each ω and h strictly positive, we have*

$$\text{cond}(M_{g,\omega}^{-1} M_\omega) \leq \sqrt{1 + g(h, \omega) [2 + g(h, \omega)^2]}$$

where

$$g(h, \omega) = \sqrt{\frac{(2 + \alpha^2)(1 + \frac{1}{h^3})^2(\frac{A}{h^2} + 1 + K)^2}{\omega^2 + (1 + \frac{1}{h^3})^2(\frac{A}{h^2} + 1 + K)^2}}$$

Proof: In the space $[m_{h,\ell}]^\perp$, we have: $D = R + \alpha Id$, where Id is the eye matrix on space $[m_{h,\ell}]^\perp$ and R is the matrix associated to the operator $-m_\ell \wedge$. Moreover, for every U in $[m_{h,\ell}]^\perp$, we have

$$(HU, m_{h,\ell}) = (U, Hm_{h,\ell}) = 0,$$

this implies, by breaking off of the elements of $[m_{h,\ell}]^\perp$, that HU is an element of $[m_{h,\ell}]^\perp$. We remark also that by working in $[m_{h,\ell}]^\perp$, we have

$$R^2 = -Id.$$

Then, we have

$$M_{g,\omega}^{-1}M_\omega = (i\omega H^{-1} - Id)H^{-1}NH,$$

where

$$N_h = -RH + (1 - \alpha)H = NH.$$

Then, for every V in $[m_{h,\ell}]^\perp$, we have the following relation

$$M_{g,\omega}^{-1}M_\omega V.M_{g,\omega}^{-1}M_\omega V = \|V\|^2 + 2\mathcal{R}[V.M_{g,\omega}^{-1}N_h V] + \|M_{g,\omega}^{-1}N_h V\|^2.$$

We designate as $\mathcal{R}[z]$ the real part of a complex number z .

Furthermore, we have the following estimations:

$$\|(H^{-1}RH)^2\| = \|(H^{-1}R^2H)^2\| = 1,$$

this implies that $\|H^{-1}RH\| = 1$. So, using the fact than

$$H^{-1}NH = -H^{-1}RH + (1 - \alpha)Id,$$

we have

$$\|H^{-1}NH\| \leq \sqrt{2 + \alpha^2}$$

and

$$\|M_{g,\omega}^{-1}\| = \max_{j \in N_h^\perp} \left(\frac{\omega^2}{\lambda_j^2} + 1 \right)^{-1} \leq g(h, \omega).$$

where λ_j is the eigenvalues of the matrix H in $[m_{\ell,h}]^\perp$ and N_h^\perp is the set of indices of $[m_{\ell,h}]^\perp$.

Then, using the lowest eigenvalue controlled by projection part of the preconditioner we conclude the proof of the Theorem.

Finally, we have the good behaviour of the preconditioned system when the mesh length h tends to 0:

$$\lim_{h \rightarrow 0} (M_{g,\omega}^{-1}M_\omega) \leq 1 + \sqrt{2 + \alpha^2},$$

This version of the preconditioner gives excellent control of the conditioning number but needs the inversion of a full matrix. This leads us to the second stage in which we will replace the complete operator H_h by its laplacian part.

3.5 Preconditioning by the Laplacian component: the direct approach

The Laplacian part of H_h is the most punitive part of the matrix M_ω in terms of preconditioning. The idea in this section is to develop an approximate conditioner $M_{g,\omega,\Delta}$ built on the operator

$$i\omega - A\Delta_h - B.$$

The matrix $M_{g,\omega,\Delta}$ is a band matrix which could be more easily handled than $M_{g,\omega}$, the earlier version of the preconditioner. This approximation of the preconditioner $M_{g,\omega}$ will be all the more accurate as the norms of the operators H_d and H_a are dominated by $\frac{A}{h^2}$. As seen in Fig. 3, the clustering of the singular value decomposition obtained for the system preconditioned by $M_{g,\omega,\Delta}$ is good. The convergence of the CNG algorithm

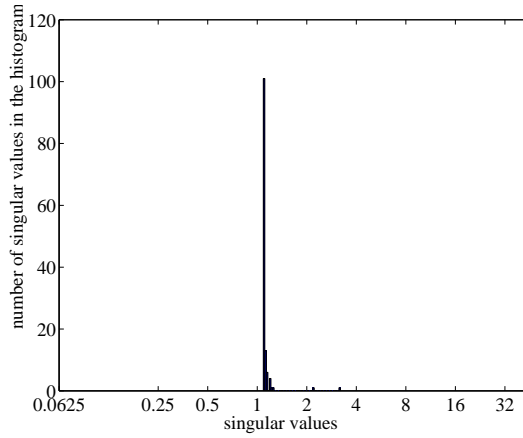


Figure 3: Singular value decomposition of the system preconditioned by $M_{g,\omega,\Delta}$.

using this method is very good: 7 iterations for ω_{min} and 9 iteration for ω_{max} (see Fig. 4).

3.6 The approximated preconditioner

Nevertheless, the use of the pre-conditioner $M_{g,\omega,\Delta}$ stays expansive. The solution is to build an easily invertible approximation of $M_{g,\omega,\Delta}$. Here we will use here the work of [12]. The idea is to project the matrix $M_{g,\omega,\Delta}$ into the circulant matrix space in the sense of the Froebenius norm.

Given a circulant matrix C n by n on \mathbb{C} generated by c , vector of \mathbb{C}^n , we have

$$\forall (i, j) \in \{1, \dots, n\}^2 \text{ and } p \in \{1, \dots, n\}, C_{i,j} = c_p \text{ if } j - i = p - 1 \text{ or } j - i = n - p + 1.$$

Then, as shown in [12], for every matrix M n by n on \mathbb{C} , the projection C of M on the

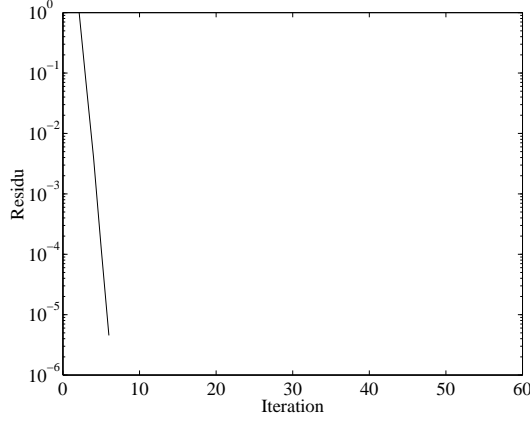


Figure 4: Residue of the system preconditionned by $M_{g,\omega,\Delta}$.

space of the circulant matrices of order n is generated by the vector c given by

$$\forall p \in \{1, \dots, n\}, c_p = \frac{1}{n} \left(\sum_{l=1}^{n-p+1} M_{l,l-p+1} + \sum_{l=n-p+2}^n M_{l,l+n-p+1} \right)$$

The three dimensional projection is more complex but the main idea is contained in the one-dimensional projection.

When the circulant approximation matrix is built, the inversion is performed in the Fourier space (the matrix produced is block-diagonal 3×3 in Fourier space), then the preconditioning is of complexity $O(N \log(N))$ for each iteration of the inversion method. The other main advantage of the method is that the storage is reduced to $O(N)$.

In this section, we have to keep in mind that the structure is a three dimensional one: the considered matrices are 3 level block matrices. This implies that the projection must be performed on the 3 levels block circulant matrices.

In the small example presented to illustrate the paper, the system preconditioned by the approximated preconditioner converges in 30 iterations for the smaller frequency and 26 iterations for the highest (see Fig. 6). The convergence curve is very good in the sense that the slope is quasi-constant. This point is quite important: susceptibility computations do not need high numerical accuracy. Effectively, the results obtained will be compared to experimental results for which the error is quite important. This comes from the fact that the samples used for experiments are far to be perfect and that the measurement tools do not have very high precision for this type of experiment.

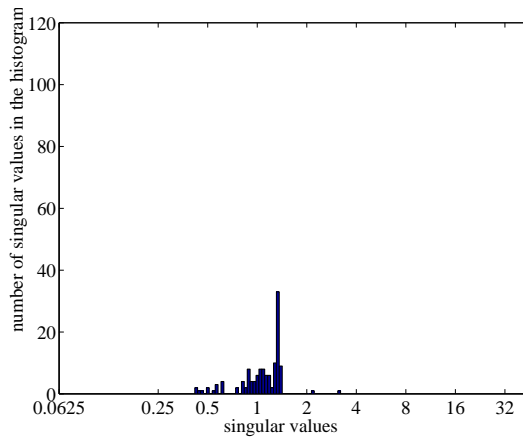


Figure 5: Singular value decomposition of the system preconditioned by the circulant approximation of $M_{g,\omega,\Delta}$.

4 Numerical simulations

We present here the number of iterations for the simulation of a ferromagnetic dot. This dot is meshed by a regular grid, size $64 \times 64 \times 32$. In this monolith a cylinder with the axis z and a circular basis (32 cells for the z direction and 64×64 for the others) is included. The total number of degrees of freedom is 393216. The results shown here have been computed on the parallel machines of ONERA and Dassault Aviation.

4.1 Parallel implementation

There are two possible levels of parallelisation for this problem: local parallelisation for computations of each iteration and global parallelisation of the frequency computations.

The global parallelisation is a repartition of each frequency computation through the processors. A main process distributes the computation to each processor such that each processor is always occupied. This part is implemented using MPI.

The local implementation, not used for the results presented here, is the parallelisation of the total magnetic field over the domain. In this computation, one part is more expensive than the others: the demagnetisation field. In fact, the computation of demagnetisation is accelerated by using its Toeplitz structure (see [8]). This computation strategy uses 3 dimensional FFT intensively. To enhance the performance, we have to parallelise the FFT computation. To do so, we have chosen to use OPEN-MP. This choice avoids the transposition of the data via the cluster that must be performed while using a distributed memory system. The results are very satisfying: for a cubic structure and sufficient number of cells (for instance a $32 \times 32 \times 32$ mesh), the computation time of FFT is divided by 1.9 on a node of two processors.

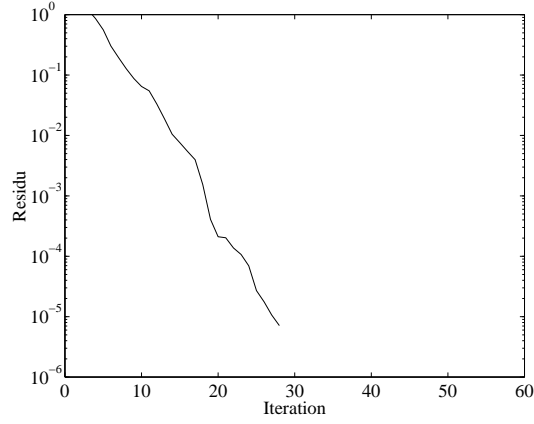


Figure 6: Residu of the system preconditioned by the circulant approximation $M_{g,\omega,\Delta}$.

4.2 Description of the benchmark statistics and results

The aim is to compute the susceptibility of a cylinder of permalloy (see for example [13] for this type of results). The parameters of the material are the following:

Parameter	Value
A	$0.17875 \cdot 10^{-11}$
α	0.05

In the following table 1, we give the number of iterations for directions x and y . The direction z in this computation is omitted because there is no resonance in this direction.

The computation has been carried out on a node composed of 8 Power4 IBM (1.1GHz) with 16 GO of Ram. An iteration takes almost 24 seconds, the complete computation took 36 hours.

$\omega/1,356$ (Hz)	iterations for x	error	iterations i for y	error
$3.00 \cdot 10^5$	57	$4.92 \cdot 10^{-2}$	127	$4.98 \cdot 10^{-2}$
$2.73 \cdot 10^5$	100	$4.85 \cdot 10^{-2}$	137	$4.91 \cdot 10^{-2}$
$2.49 \cdot 10^5$	198	$4.90 \cdot 10^{-2}$	267	$4.99 \cdot 10^{-2}$
$2.26 \cdot 10^5$	146	$4.99 \cdot 10^{-2}$	272	$4.95 \cdot 10^{-2}$
$2.06 \cdot 10^5$	188	$4.99 \cdot 10^{-2}$	329	$4.90 \cdot 10^{-2}$
$1.88 \cdot 10^5$	290	$4.96 \cdot 10^{-2}$	356	$4.91 \cdot 10^{-2}$
$1.71 \cdot 10^5$	316	$4.99 \cdot 10^{-2}$	317	$4.85 \cdot 10^{-2}$
$1.55 \cdot 10^5$	326	$4.98 \cdot 10^{-2}$	386	$4.94 \cdot 10^{-2}$
$1.41 \cdot 10^5$	390	$4.99 \cdot 10^{-2}$	355	$4.94 \cdot 10^{-2}$
$1.29 \cdot 10^5$	298	$5.00 \cdot 10^{-2}$	376	$4.97 \cdot 10^{-2}$
$1.17 \cdot 10^5$	329	$4.88 \cdot 10^{-2}$	354	$4.88 \cdot 10^{-2}$

$\omega/1,356$ (Hz)	iterations for x	error	iterations i for y	error
$1.07 \cdot 10^5$	490	$4.97 \cdot 10^{-2}$	286	$4.93 \cdot 10^{-2}$
$9.71 \cdot 10^4$	615	$4.91 \cdot 10^{-2}$	400	$5.00 \cdot 10^{-2}$
$8.84 \cdot 10^4$	664	$4.99 \cdot 10^{-2}$	504	$4.95 \cdot 10^{-2}$
$8.05 \cdot 10^4$	638	$4.94 \cdot 10^{-2}$	416	$4.81 \cdot 10^{-2}$
$7.33 \cdot 10^4$	436	$4.94 \cdot 10^{-2}$	371	$4.92 \cdot 10^{-2}$
$6.67 \cdot 10^4$	318	$4.96 \cdot 10^{-2}$	319	$4.70 \cdot 10^{-2}$
$6.07 \cdot 10^4$	291	$4.98 \cdot 10^{-2}$	294	$4.92 \cdot 10^{-2}$
$5.53 \cdot 10^4$	351	$4.85 \cdot 10^{-2}$	266	$4.91 \cdot 10^{-2}$
$5.03 \cdot 10^4$	377	$4.91 \cdot 10^{-2}$	258	$4.78 \cdot 10^{-2}$
$4.58 \cdot 10^4$	433	$4.99 \cdot 10^{-2}$	252	$4.96 \cdot 10^{-2}$
$4.17 \cdot 10^4$	480	$4.97 \cdot 10^{-2}$	248	$4.85 \cdot 10^{-2}$
$3.79 \cdot 10^4$	543	$4.91 \cdot 10^{-2}$	247	$4.75 \cdot 10^{-2}$
$3.45 \cdot 10^4$	592	$4.95 \cdot 10^{-2}$	248	$5.00 \cdot 10^{-2}$
$3.14 \cdot 10^4$	547	$4.99 \cdot 10^{-2}$	248	$4.91 \cdot 10^{-2}$
$2.86 \cdot 10^4$	549	$4.86 \cdot 10^{-2}$	248	$5.00 \cdot 10^{-2}$
$2.61 \cdot 10^4$	571	$4.93 \cdot 10^{-2}$	247	$4.97 \cdot 10^{-2}$
$2.37 \cdot 10^4$	618	$4.99 \cdot 10^{-2}$	243	$4.99 \cdot 10^{-2}$
$2.16 \cdot 10^4$	653	$4.90 \cdot 10^{-2}$	244	$4.99 \cdot 10^{-2}$
$1.97 \cdot 10^4$	686	$4.62 \cdot 10^{-2}$	247	$4.92 \cdot 10^{-2}$
$1.79 \cdot 10^4$	723	$4.83 \cdot 10^{-2}$	251	$4.92 \cdot 10^{-2}$
$1.63 \cdot 10^4$	779	$4.90 \cdot 10^{-2}$	254	$4.97 \cdot 10^{-2}$
$1.48 \cdot 10^4$	839	$4.94 \cdot 10^{-2}$	257	$4.99 \cdot 10^{-2}$
$1.35 \cdot 10^4$	855	$4.90 \cdot 10^{-2}$	265	$4.86 \cdot 10^{-2}$
$1.23 \cdot 10^4$	842	$4.99 \cdot 10^{-2}$	267	$4.95 \cdot 10^{-2}$
$1.12 \cdot 10^4$	832	$4.90 \cdot 10^{-2}$	273	$4.95 \cdot 10^{-2}$
$1.02 \cdot 10^4$	832	$4.94 \cdot 10^{-2}$	279	$4.96 \cdot 10^{-2}$
$9.27 \cdot 10^3$	835	$4.92 \cdot 10^{-2}$	280	$4.98 \cdot 10^{-2}$
$8.44 \cdot 10^3$	691	$4.92 \cdot 10^{-2}$	289	$4.89 \cdot 10^{-2}$
$7.68 \cdot 10^3$	843	$4.96 \cdot 10^{-2}$	292	$4.94 \cdot 10^{-2}$
$6.99 \cdot 10^3$	856	$4.98 \cdot 10^{-2}$	296	$4.97 \cdot 10^{-2}$
$6.36 \cdot 10^3$	868	$4.90 \cdot 10^{-2}$	302	$5.00 \cdot 10^{-2}$
$5.79 \cdot 10^3$	875	$4.93 \cdot 10^{-2}$	305	$4.94 \cdot 10^{-2}$
$5.27 \cdot 10^3$	888	$4.83 \cdot 10^{-2}$	311	$4.95 \cdot 10^{-2}$
$4.80 \cdot 10^3$	893	$4.98 \cdot 10^{-2}$	316	$4.99 \cdot 10^{-2}$
$4.37 \cdot 10^3$	907	$4.94 \cdot 10^{-2}$	319	$4.94 \cdot 10^{-2}$
$3.98 \cdot 10^3$	913	$4.92 \cdot 10^{-2}$	327	$4.94 \cdot 10^{-2}$
$3.62 \cdot 10^3$	923	$4.97 \cdot 10^{-2}$	328	$4.99 \cdot 10^{-2}$
$3.30 \cdot 10^3$	944	$4.99 \cdot 10^{-2}$	336	$4.91 \cdot 10^{-2}$
$3.00 \cdot 10^3$	951	$4.85 \cdot 10^{-2}$	339	$4.94 \cdot 10^{-2}$

Table 1: Iteration table.

5 Conclusion

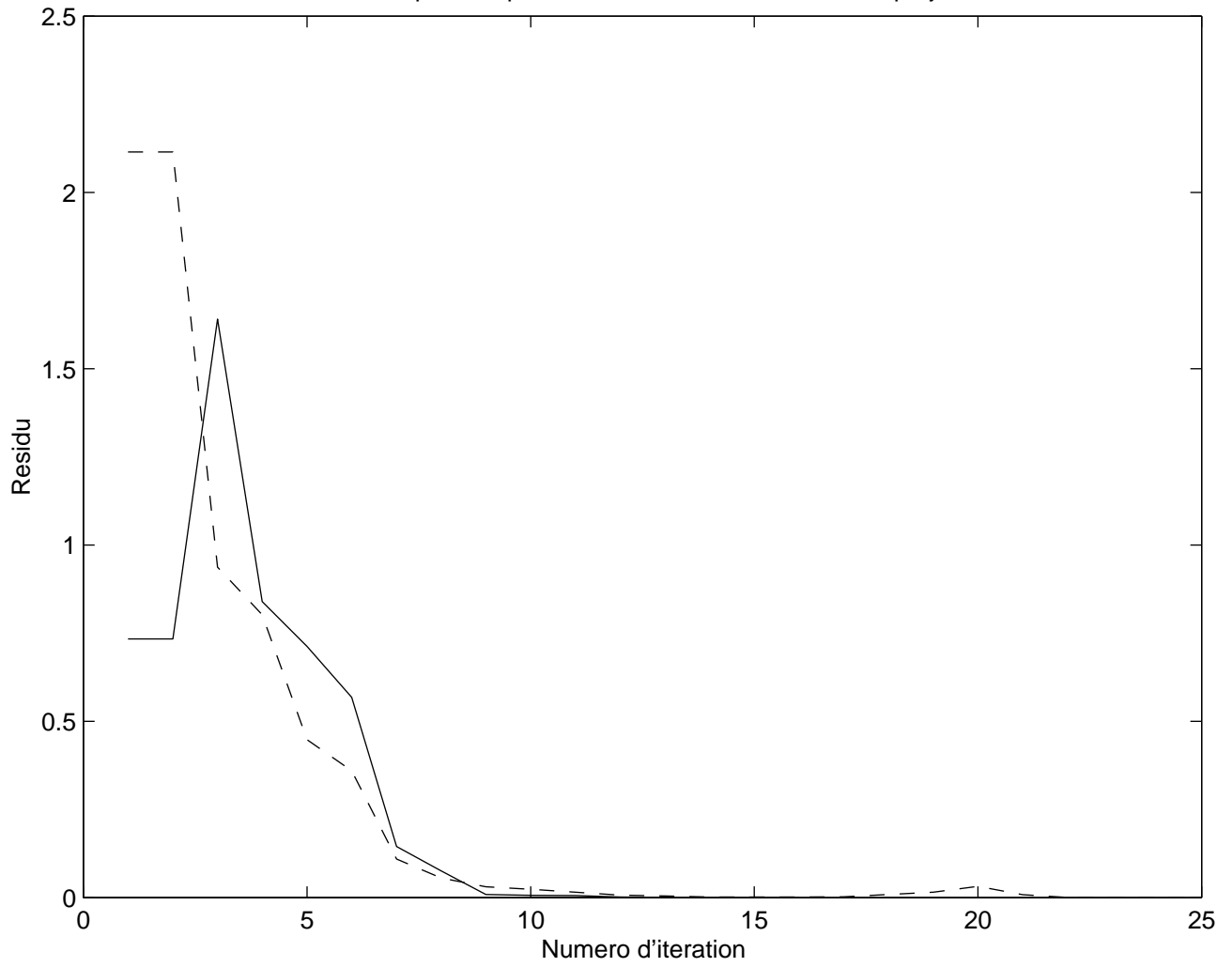
The goal of the study was to allow the computing of micro-wave susceptibility of ferromagnetic particles with thin details. This last point called for very large meshes (about 300000 degrees of freedom) for which the classical inversion methods with no preconditioning did not work at all, or required such a large amount of iterations that the computation times for an acceptable range of frequencies was far from useful. The strategy presented in this article is an industrial computations approach, and obtains interesting results for a large spectrum of benchmark. Computations of realistic experiments have been performed (see [14, 13, 15]) for physical systems where it was possible to compare results with physical experiments. Some problems remain, in particular, the strategy developed aims at the laplacian part of the total magnetic field whereas some systems are revealed to be principally influenced by the demagnetising field. The next step is to extend the strategy of the paper in order to include the demagnetisation part of the magnetic field in the approximated preconditioner. The main difficulty of the extension is algorithmic: to build a good circulant approximation of block Toeplitz matrices. An another interesting point to study would be the implementation of an efficient parallelised FFT algorithm for distributed memory systems. The main problem of such an implementation would be the optimisation of the transposition phase of the data through the memory nodes of the distributed system.

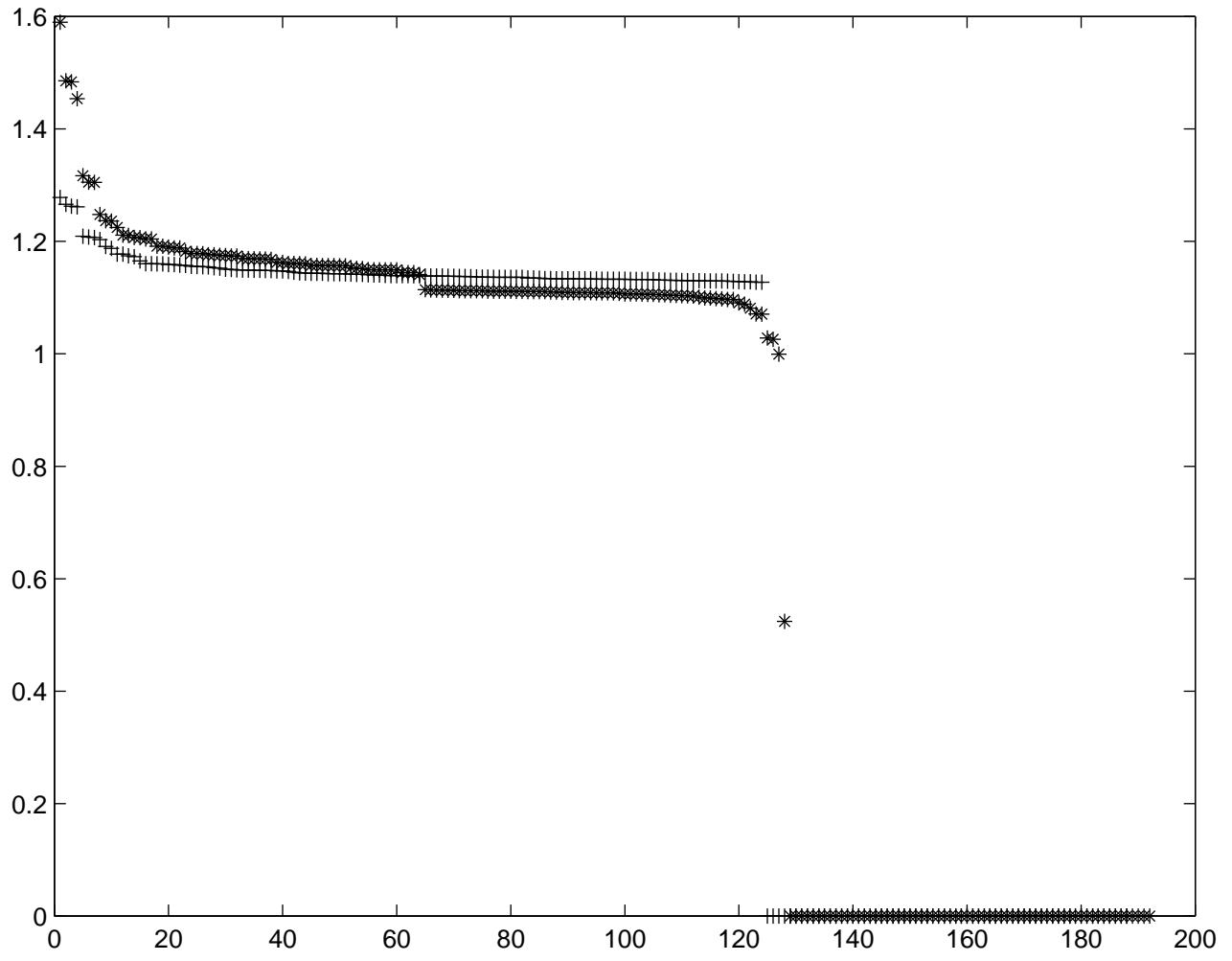
References

- [1] W. F. Brown. *Micromagnetics*. Interscience Publishers, 1963.
- [2] W. F. Brown. *Magnetostatic Principles in Ferromagnetism*. North-Holland, 1962.
- [3] F. Alouges. *Mémoire d'habilitation à diriger des recherches*. PhD thesis, Université Paris 11, 1999.
- [4] A. Bagnérés-Viallix, P. Baras, and J.B. Albertini. 2d and 3d calculations of micro-magnetic wall structures using finite elements. *IEEE Transactions on Magnetics*, 27(5):3819–3822, September 1991.
- [5] M. E. Schabes and H. N. Bertram. Magnetization processes in ferromagnetic cubes. *Journal of Applied Physics*, 1:1347–1357, August 1988.
- [6] J. Miltat, G. Albuquerque, and A. Thiaville. Micromagnetics: Dynamical aspects. *Lecture Notes in Physics*, 565, 2001.
- [7] S. Labbé and P.Y. Bertin. Microwave polarisability of ferrite particles with non-uniform magnetization. *Journal of Magnetism and Magnetic Materials*, 206:93–105, 1999.
- [8] S. Labbé. Fast computation for large magnetostatic systems adapted for micro-magnetism. *SISC*, (to appear), 2005.

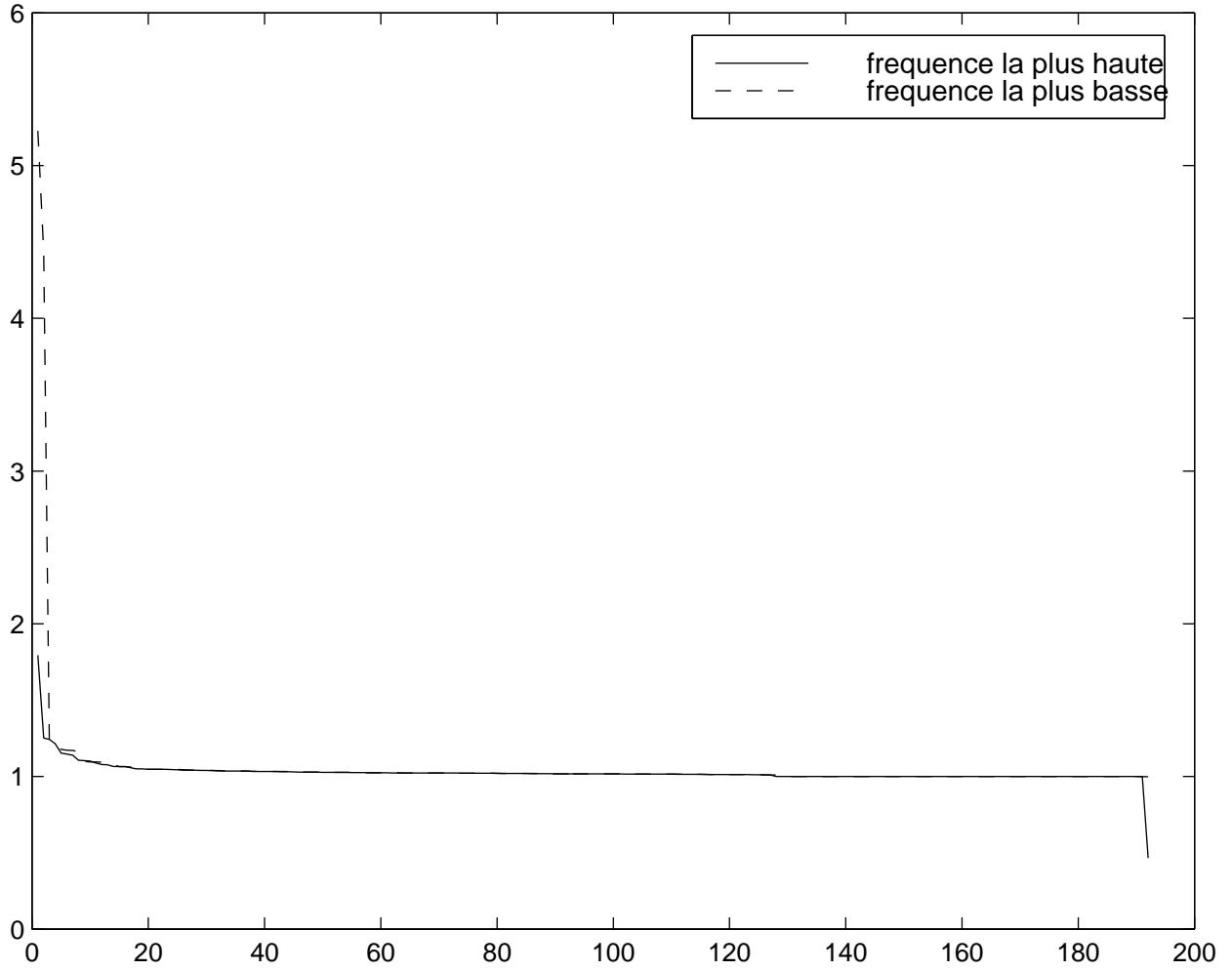
- [9] S. Labbé. *Simulation numérique du comportement hyperfréquence des matériaux ferromagnétiques*. PhD thesis, Université Paris 13, December 1998.
- [10] L. Halpern and S. Labbé. Modélisation et simulation du comportement des matériaux ferromagnétiques. *Matapli*, 66:70–86, 2001.
- [11] N. M. Nachtigal, S. C. Reddy, and L. N. Trefethen. How fast are nonsymmetric matrix iterations ? *SIAM J. Matrix Anal. Appl.*, 13(3):778–795, 1992.
- [12] E. E Tyrtshnikov. Optimal and super optimal circulant preconditionners. *Matrix Anal. Appl.*, (2):459–473, April 1992.
- [13] F. Boust, N. Vukadinovic, and S. Labbé. High-frequency susceptibility of soft ferromagnetic nanodots. *J. Magn. Magn. Mat.*, 272-276:708–710, 2004.
- [14] C. Vaast-Paci and L. Leylekian. Numerical simulations of isolated particles susceptibilities: effects of shape and size. *J. Magn. Magn. Mat.*, 237:342–352, 2001.
- [15] F. Boust and N. Vukadinovic. Micromagnetic simulations of vortex-state excitations in soft magnetic nanostructures. *Phys. Rev. B*, 70:172408, 2004.

Relaxation pour un preconditionnement circulant sans projection

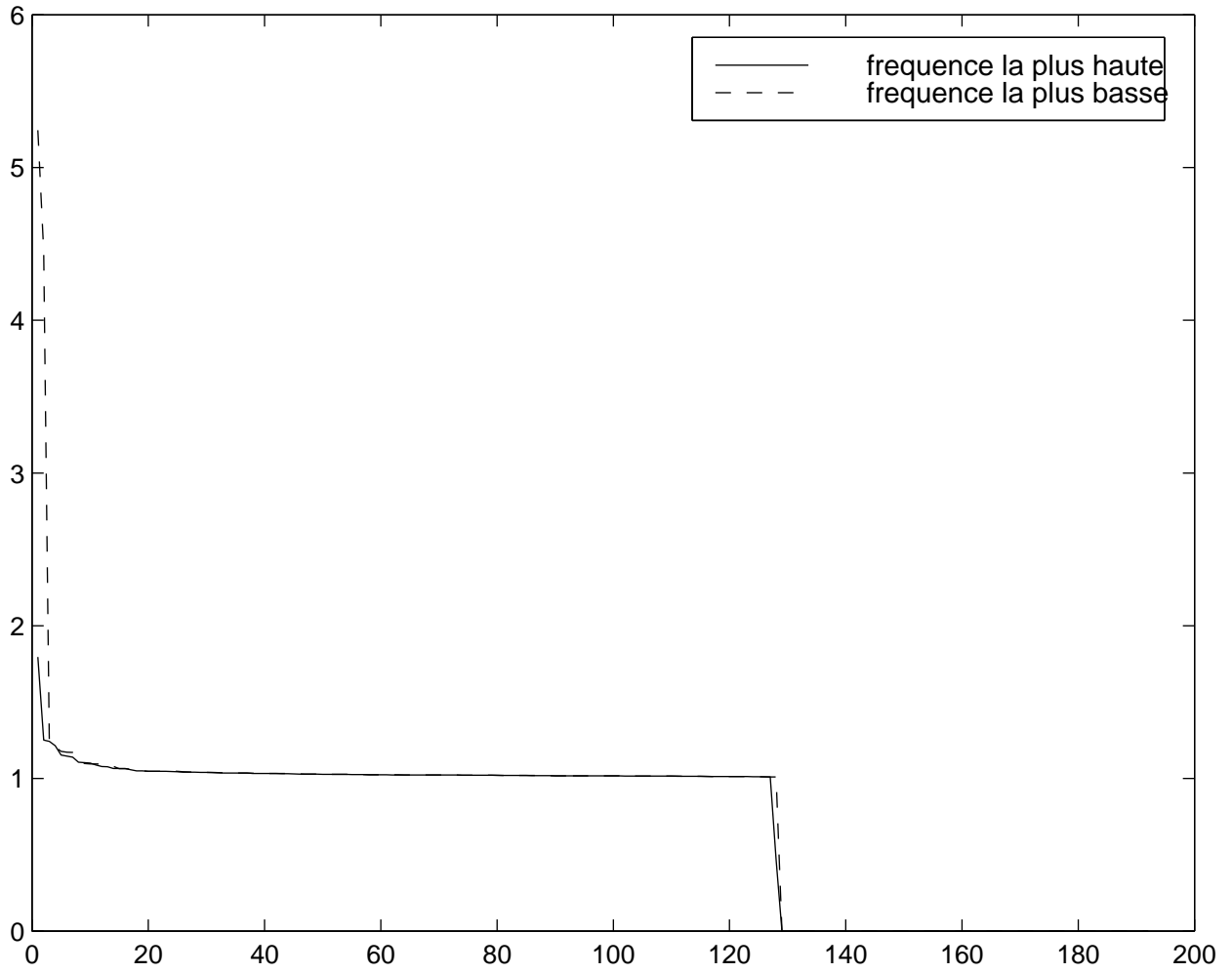




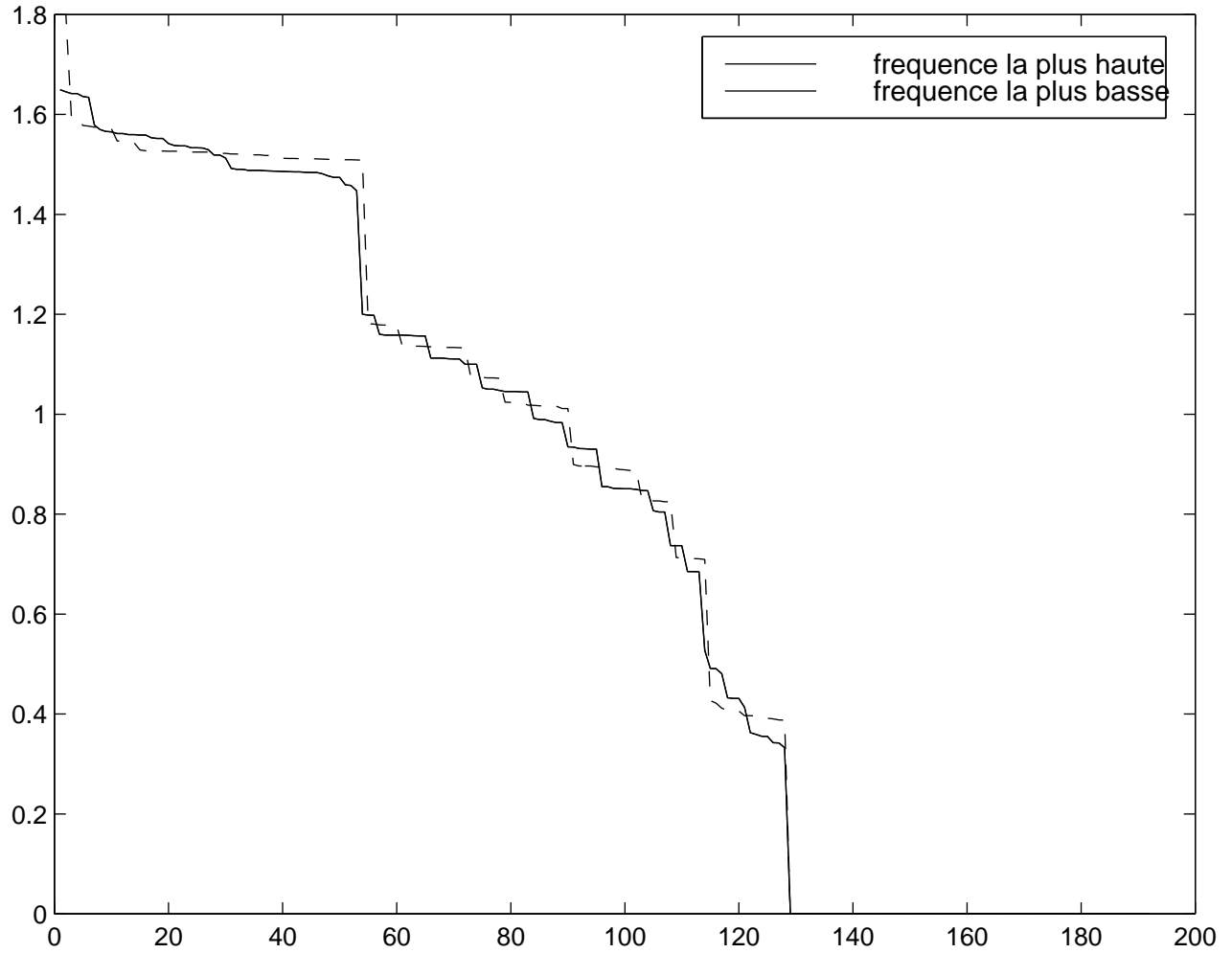
Decomposition en valeur singulieres de la matrice non projetee preconditionnee



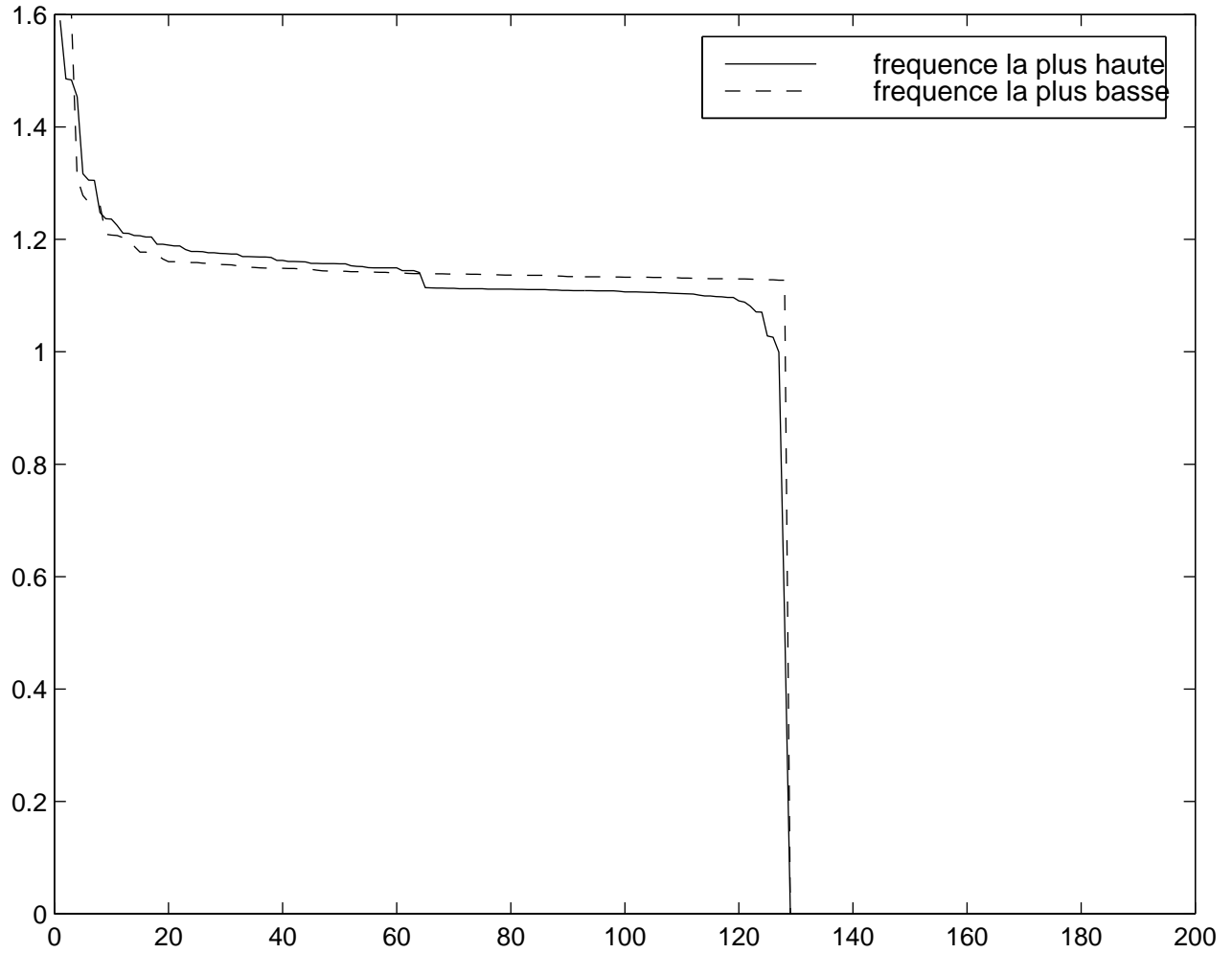
Decomposition en valeur singulieres de la matrice projetee preconditionnee



Decomposition en valeur singulieres de la matrice projetee preconditionnee



Decomposition en valeur singulieres de la matrice projetee preconditionnee



Decomposition en valeur singulieres de la matrice projetee

